

# Polynomial Networks in Deep Classifiers

Grigoris G Chrysos<sup>1</sup> Markos Georgopoulos<sup>2</sup> Jiankang Deng<sup>2</sup> Yannis Panagakis<sup>3</sup>

## Abstract

Deep neural networks have been the driving force behind the success in classification tasks, e.g., object and audio recognition. Impressive results and generalization have been achieved by a variety of recently proposed architectures, the majority of which are seemingly disconnected. In this work, we cast the study of deep classifiers under a unifying framework. In particular, we express state-of-the-art architectures (e.g., residual and non-local networks) in the form of different degree polynomials of the input. Our framework provides insights on the inductive biases of each model and enables natural extensions building upon their polynomial nature. The efficacy of the proposed models is evaluated on standard image and audio classification benchmarks. The expressivity of the proposed models is highlighted both in terms of increased model performance as well as model compression. Lastly, the extensions allowed by this taxonomy showcase benefits in the presence of limited data and long-tailed data distributions. We expect this taxonomy to provide links between existing domain-specific architectures.

## 1. Introduction

The unprecedented performance of AlexNet (Krizhevsky et al., 2012) in ImageNet classification (Russakovsky et al., 2015) led to the resurgence of research in the field of neural networks. Since then, an extensive corpus of papers has been devoted to improving classification performance by modifying the architecture of the neural network. However, only a handful (of seemingly disconnected) architectures, such as ResNet (He et al., 2016) or non-local neural networks (Wang et al., 2018b), have demonstrated impressive generalization across different tasks (e.g., (Zhang et al.,

<sup>\*</sup>Equal contribution <sup>1</sup>Department of Electrical Engineering, Ecole Polytechnique Federale de Lausanne (EPFL) <sup>2</sup>Department of Computing, Imperial College London, United Kingdom <sup>3</sup>Department of Informatics and Telecommunications, University of Athens. Correspondence to: Grigoris G Chrysos <grigoris.chrysos@epfl.ch>.

Preliminary work. Under review. Copyright 2021 by the author(s).

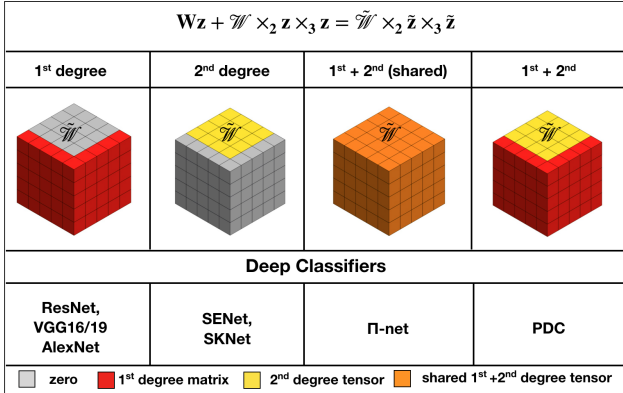


Figure 1. Parameter interactions for different degrees of polynomials. For visualization purpose we assume a second-degree expansion, where we have folded the learnable parameters into a tensor  $\tilde{W}$  and the input is vectorized. The equation on the top is the second-degree polynomial in a tensor-format, while the  $\tilde{z}$  is a padded version of  $z$  as demonstrated in the supplementary. Notice that first-degree polynomials (He et al., 2016; Krizhevsky et al., 2012; Simonyan & Zisserman, 2015) have zeros in a large part of the tensor  $\tilde{W}$ , while similarly second-degree polynomials (Hu et al., 2018b; Li et al., 2019) have the matrices connected to first-order interactions zero. On the contrary,  $\Pi$ -nets along with the proposed PDC capture both interactions. Importantly, we illustrate how PDC learns a more expressive model without the enforced sharing of the  $\Pi$ -net. The derivation is deferred to the supplementary.

2019)), domains (e.g., (Won et al., 2019)) and modalities (e.g., (Kim et al., 2018)). This phenomenon can be attributed to the challenging nature of devising a network and the lack of understanding regarding the assumptions that come with its design, i.e., its inductive bias.

Demystifying the success of deep neural architectures is of paramount importance. In particular, significant effort has been devoted to the study of neural architectures, e.g., depth versus width of the neural network (Rolnick & Tegmark, 2018; Hanin, 2019) and the effect of residual connections on the training of the network (Hardt & Ma, 2017; Huang et al., 2017; He et al., 2016). In this work, we offer a principled approach to study state-of-the-art classifiers as polynomial expansions. We show that polynomials have been a recurring theme in numerous classifiers and interpret their design choices under a unifying framework.

The proposed framework provides a taxonomy for a collection of deep classifiers, e.g., non-local neural networks is a third-degree polynomial and ResNet is a first-degree polynomial. Thus, we provide an intuitive way to study and extend existing networks, as well as interpret their gap in performance. Lastly, we design extensions on existing methods and show that we can improve their classification accuracy or achieve parameter reduction. Concretely, our contributions are the following:

- We express a collection of state-of-the-art neural architectures as polynomials. Our unifying framework sheds light on the inductive bias of each architecture. We experimentally verify the performance of different methods of the taxonomy on four standard benchmarks.
- Our framework allows us to propose intuitive modifications on existing architectures. The proposed new architectures consistently improve upon their corresponding baselines, both in terms of accuracy as well as model compression.
- We evaluate the performance under various changes in the training distribution, i.e., limiting the number of samples per class or creating a long-tailed distribution. The proposed models improve upon the baselines in both cases.
- We release the code as open source to enable the reproduction of our results.

## 2. Polynomials and deep classifiers

The proposed framework unifies recent deep classifiers through the lens of polynomials. We begin by providing an intuitive explanation on how a polynomial expansion emerges on various types of variables and then formalize the concept on different degrees of polynomial expansion. Below, we symbolize matrices (vectors) with bold capital (lower) letters, e.g.  $\mathbf{X}(x)$ . A variable that can be either a matrix or a vector is denoted by  $\hat{Z}$ .

Polynomials express a relationship between an input variable (e.g., a scalar  $z$ ) and (learnable) coefficients; this relationship only involves the two core operations of addition and multiplication. When the input variable is in vector form, e.g.,  $\mathbf{z} \in \mathbb{R}^\delta$  with  $\delta \in \mathbb{N}$ , then the polynomial captures the relationships between the different elements of the input vector. The input variable also be a higher-dimensional structure, e.g., a matrix. This is frequently the case in computer vision, where one dimension can express spatial dimensions, while the other can express the features (channels). The polynomial can either capture the interactions across every element of the matrix with every other element, or it can have higher-order interactions between

specific elements, e.g., the interactions of a row with each column.

We formalize the framework of polynomials below. Formally, let functions  $\Phi_i^{[d]}(\hat{Z})$  define a linear (or multi-linear) function over  $\hat{Z}$ . The input variable  $\hat{Z}$  can either be a vector or a matrix, while  $d$  declares the degree and  $i$  the index of the function. Then, a polynomial of degree  $-N$  is expressed as:

$$\hat{Y} = \hat{\beta} + \Phi_1^{[1]}(\hat{Z}) + \Phi_1^{[2]}(\hat{Z})\Phi_2^{[2]}(\hat{Z}) + \dots + \underbrace{\Phi_1^{[N]}(\hat{Z}) \dots \Phi_{N-1}^{[N]} \Phi_N^{[N]}(\hat{Z})}_{N \text{ terms}} \quad (1)$$

where  $\hat{\beta}$  is the constant term. Evidently, each additional degree introduces new parameters that can grow up to exponentially with respect to the degree. However, we posit that this introduces a needed inductive bias on the method. In addition, if reduced parameters are required, this can be achieved by using low-rank assumptions or by sharing parameters across different degrees.

Using the formulation in (1), we exhibit how well-established methods can be formulated as polynomials. We present a taxonomy of classifiers based on the degree of the polynomial. In particular, we present first, second, third and higher-degree polynomial expansions. For modeling purposes, we focus on the core block of each architecture, while ignoring any activation functions.

**First-degree polynomials** include the majority of the feed-forward networks, such as AlexNet (Krizhevsky et al., 2012), VGG (Simonyan & Zisserman, 2015). Specifically, the networks that include stacked linear operations (fully-connected or convolutional layers) but do not include any matrix or elementwise multiplication of the representations fit in this category. Such networks can be expressed in the form  $\hat{Y} = \mathbf{C}\hat{Z} + \hat{\beta}$ , where the weight matrix  $\mathbf{C}$  is a learnable parameter. A special case is ResNet (He et al., 2016). The idea is to introduce shortcut connections that enable residual learning. Notation-wise this is a re-parametrization of the weight matrix  $\mathbf{C}$  as  $\hat{Y}_r = (\mathbf{I} + \mathbf{C})\hat{Z} + \hat{\beta}$  where  $\mathbf{I}$  is an identity matrix. Thus,  $\Phi_1^{[1]}(\hat{Z}) = (\mathbf{I} + \mathbf{C})\hat{Z}$ .

**Second-degree polynomials** model self-interactions, i.e., they can selectively maximize the related inputs through second-order interactions. Often the interactions emerge in a particular dimension, e.g., correlations of the channels only, based on the particular application.

One special case of the second-degree polynomial is the *Squeeze-and-excitation networks (SENet)* (Hu et al., 2018b). The motivation lies in improving the channel-wise interactions, since there is already a strong inductive bias for the spatial interactions through convolutional layers. Notation-

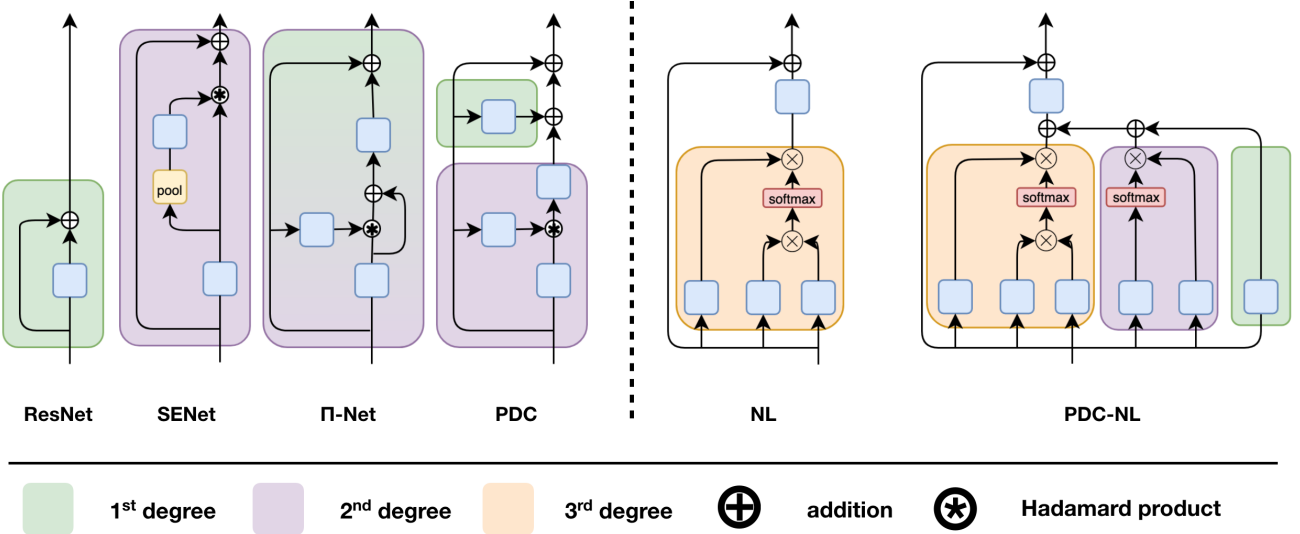


Figure 2. Blocks (up to third-degree) from different architectures. The layers (i.e., blue boxes) denote any linear operation, e.g., a convolution or a fully-connected layer, depending on the architecture. From left to right, the degree of the polynomial is increasing. Our framework enables also to complete the missing terms of the polynomial (i.e., PDC-NL versus NL).

wise, the squeeze-and-excitation block is expressed as  $\mathbf{Y}_s = (\mathbf{Z}\mathbf{C}_1) * r(p(\mathbf{Z}\mathbf{C}_1)\mathbf{C}_2)$ , where  $*$  denotes the Hadamard product,  $p$  is the global pooling function,  $r$  is a function that replicates the channels in the spatial dimensions and  $\mathbf{C}_1, \mathbf{C}_2$  are weight matrices with learnable parameters. For simplicity, we assume the input is a matrix instead of a tensor, i.e.,  $\mathbf{Z} \in \mathbb{R}^{hw \times c}$  with  $h$  the height,  $w$  the width and  $c$  the channels of the image. Then,  $\mathbf{Y}_s$  expresses a second-degree term with  $\Phi_1^{[2]}(\mathbf{Z}) = \mathbf{Z}\mathbf{C}_1$  and  $\Phi_2^{[2]}(\mathbf{Z}) = \frac{1}{hw}\mathbf{I} \times_3 (\mathbf{C}_2^T \mathbf{C}_1^T \mathbf{Z}^T \vec{\mathbf{1}})$  where  $\mathbf{I}$  is a third-order super-diagonal unit tensor and  $\vec{\mathbf{1}}$  is a vector of ones. The proof is deferred to the supplementary. The selective kernels networks (Li et al., 2019) introduce a variant, where  $\mathbf{Z}$  is replaced with the transformed  $\mathbf{Z}\mathbf{U}_1 + \mathbf{Z}\mathbf{U}_2$ . The learnable parameters  $\mathbf{U}_1, \mathbf{U}_2$  include different receptive fields. However, the degree of the polynomial remains the same, i.e., second-degree.

**Third-degree polynomials** can encode long-range dependencies that are not captured by local operators, such as convolutions. A popular framework in this category is the *non-local neural networks (NL)* (Wang et al., 2018b). The non-local block can be expressed as:  $\mathbf{Y}_n = (\mathbf{Z}\mathbf{C}_1\mathbf{C}_2\mathbf{Z}^T)\mathbf{Z}\mathbf{C}_3$  where the matrices  $\mathbf{C}_i$  for  $i = 1, 2, 3$  are learnable parameters and  $\mathbf{Z} \in \mathbb{R}^{hw \times c}$  is the input. The third-degree term is then  $\Phi_1^{[3]}(\mathbf{Z}) = \mathbf{Z}\mathbf{C}_1$ ,  $\Phi_2^{[3]}(\mathbf{Z}) = \mathbf{C}_2\mathbf{Z}^T$  and  $\Phi_3^{[3]}(\mathbf{Z}) = \mathbf{Z}\mathbf{C}_3$ . Recently, *disentangled non-local networks (DNL)* (Yin et al., 2020) extends the formulation by including a second-degree term and the generated output is  $\mathbf{Y}_{dn} = ((\mathbf{Z}\mathbf{C}_1 - \mu_q)(\mathbf{C}_2\mathbf{Z} - \mu_k)^T + \mathbf{Z}\mathbf{c}_4\vec{\mathbf{1}}^T)\mathbf{Z}\mathbf{C}_3$  where  $\mathbf{c}_4$  is a weight vector,  $\mu_q, \mu_k$  are the mean vectors of the

keys and queries representations and  $\vec{\mathbf{1}} \in \mathbb{R}^{hw \times 1}$  a vector of ones. This translates to a new second-degree term with  $\Phi_1^{[2]}(\mathbf{Z}) = \mathbf{Z}\mathbf{c}_4\vec{\mathbf{1}}^T$  and  $\Phi_2^{[2]}(\mathbf{Z}) = \mathbf{Z}\mathbf{C}_3$ .

**Higher-degree polynomials** can (virtually) approximate any smooth functions. The Weierstrass theorem (Stone, 1948) and its extension (Nikol'skii, 2013) (pg 19) guarantee that any smooth function can be approximated by a higher-degree polynomial.

A recently proposed framework that leverages high-degree polynomials to approximate functions is *Pi-net* (Chrysos et al., 2020). Each *Pi*-net block is a polynomial expansion with a pre-determined degree. The learnable coefficients of the polynomial are represented with higher-order tensors. One of the drawbacks of this method is that the order of the tensor increases linearly with the degree, hence the parameters explode exponentially. To mitigate this issue, a coupled tensor decomposition that allows for sharing among the coefficients is utilized. Thus, the number of parameters is reduced significantly. Although the method is formulated as a complete polynomial, the proposed sharing of the coefficients suppresses its expressive power in favour of model compression. The model used for the classification can be

expressed with the following recursive relationship<sup>1</sup>:

$$\mathbf{x}_n = (\mathbf{A}_{[n]}^T \mathbf{z}) * (\mathbf{S}_{[n]}^T \mathbf{x}_{n-1} + \mathbf{B}_{[n]}^T \mathbf{b}_{[n]}) + \mathbf{x}_{n-1} \quad (2)$$

for an  $N^{th}$ -degree expansion order with  $n = 2, \dots, N$ . The weight matrices  $\mathbf{A}_{[n]}, \mathbf{S}_{[n]}, \mathbf{B}_{[n]}$  and the weight vector  $\mathbf{b}$  are learnable parameters, while  $\mathbf{x}_1 = (\mathbf{A}_{[1]}^T \mathbf{z}) * (\mathbf{B}_{[1]}^T \mathbf{b}_{[1]})$ . The recursive equation can be used to express an arbitrary degree of expansion, while the weight matrices are shared across different degree terms. For instance,  $\mathbf{A}_{[2]}$  is shared by both first and second-degree terms when  $N = 2$ .

**From blocks to architecture:** The core blocks of different architectures, and their polynomial counterparts, are analyzed above. The final network (in each case) is obtained by concatenating the respective blocks in a cascade. That is, the output of the first block is used as the input for the next block and so on. Each block expresses a polynomial expansion, thus, the final architecture expresses a product of polynomials.

**Activation functions:** The aforementioned architectures are typically used in conjunction with activation functions, e.g., non-local blocks utilize the softmax function. Activation functions enable the aforementioned architectures (especially the first-degree) to achieve universal approximation capabilities (Hornik et al., 1989). However, the works successfully modeling the activation functions are limited. Sometimes the activation functions can be omitted, or they can be absorbed in the formulation (Ma et al., 2019), however this is beyond the scope of this work.

### 3. Novel architectures based on the taxonomy

The taxonomy offers a new perspective on how to modify existing architectures in a principled way. We showcase how new architectures arise in a natural way by modifying the popular Non-local neural network and the recent  $\Pi$ -nets.

#### 3.1. Higher-degree ResNet blocks

As shown in the previous section, the ResNet block is a first-degree polynomial. We can extend the polynomial expansion degree in order to enable higher-order correlations.

<sup>1</sup>In the supplementary, we include an inductive proof of how their polynomial expansion that utilizes higher-order tensors is equivalent to (1); the idea is to convert both expansions into an element-wise format. Then, the equivalence is trivial to show and thus how to obtain the tensors from our format.

A general  $N^{th}$ -degree polynomial is expressed as<sup>2</sup>:

$$\mathbf{y} = \sum_{n=1}^N \left( \mathbf{W}^{[n]} \prod_{j=2}^{n+1} \times_j \mathbf{z} \right) + \boldsymbol{\beta} \quad (3)$$

where  $\mathbf{z} \in \mathbb{R}^\delta$ ,  $\times_m$  denotes the mode-m vector product,  $\{\mathbf{W}^{[n]} \in \mathbb{R}^{o \times \prod_{m=1}^n \times_m \delta}\}_{n=1}^N$  are the tensor parameters. To reduce the learnable parameters, we assume a low-rank CP decomposition (Kolda & Bader, 2009) on each tensor. By applying Lemma 1 (supplementary), we obtain<sup>2</sup>:

$$\mathbf{y} = \boldsymbol{\beta} + \mathbf{C}_{1,[1]}^T \mathbf{z} + \left( \mathbf{C}_{1,[2]}^T \mathbf{z} \right) * \left( \mathbf{C}_{2,[2]}^T \mathbf{z} \right) + \dots + \underbrace{\left( \mathbf{C}_{1,[N]}^T \mathbf{z} \right) * \dots * \left( \mathbf{C}_{N,[N]}^T \mathbf{z} \right)}_{N \text{ Hadamard products}} \quad (4)$$

where all  $\mathbf{C}_i$  are learnable parameters. Our proposed model in (4) is modular and can be designed for arbitrary polynomial degree. A schematic of (4) is depicted in Fig 3. The proposed model differentiates itself from (2) by not assuming any parameter sharing across the different degree terms.

#### 3.2. Polynomial non-local blocks of different degrees

In this section, we demonstrate how the proposed taxonomy can be used to design a new architecture based on non-local blocks (NL). NL includes a third-degree term, while disentangled non-local network (DNL) includes both a third-degree and a second-degree term.

We begin by including an additional first-degree term with learnable weights. The formed PDC- $NL^{[3]}$  block is:

$$\mathbf{Y}_{ours}^{[3]} = (\mathbf{Z} \mathbf{C}_1 \mathbf{C}_2 \mathbf{Z}^T) \mathbf{Z} \mathbf{C}_3 + \mathbf{Z} \mathbf{C}_4 \mathbf{Z} \mathbf{C}_5 + \mathbf{Z} \mathbf{C}_6 \quad (5)$$

where  $\mathbf{C}_i$  are learnable parameters. In practice, a softmax activation function is added for the second and third degree factors, similar to the baseline. Besides the first-degree term, the proposed model differentiates itself from DNL by removing the sharing between the factors of third and second degree (i.e.,  $\mathbf{C}_3$  and  $\mathbf{C}_5$ ) as well as utilizing a full factor matrix instead of a vector for the latter (i.e.,  $\mathbf{C}_4$ ). In our implementation the matrices  $\mathbf{C}_i$  matrices (for  $i \neq 4$ ) compress the channels of the input by a factor of 4 for all models.

Building on (5), we propose to expand the PDC- $NL^{[3]}$  to a fourth degree polynomial expansion. We multiply the right hand side of (5) with a linear function with respect to the input  $\mathbf{Z}$ . That is, the PDC- $NL^{[4]}$  block is:

$$\mathbf{Y}_{ours}^{[4]} = \mathbf{Y}_{ours}^{[3]} + \mathbf{Y}_{ours}^{[3]} * r(p(\mathbf{Z} \mathbf{C}_7) \mathbf{C}_8), \quad (6)$$

<sup>2</sup>The detailed notation and the derivation of the model is deferred to the supplementary.

where the term  $r(p(\mathbf{Z}C_7)C_8)$  is similar to squeeze-and-excitation right hand side term. The new term captures the channel-wise correlations.

## 4. Experimental evaluation

In this section, we study how the degree of the polynomial expansion affects the expressive power of the model. Our goal is to illustrate how the taxonomy enables improvements in strong-performing models with minimal and intuitive modifications. This approach should also shed light on the inductive bias of each model, as well as the reasons behind the gap in performance and model compression. Unless mentioned otherwise, the degree of the polynomial for each block is considered the second-degree expansion. The proposed variants are referred to as PDC. Experiments with higher-degree polynomials, which are denoted as  $\text{PDC}^{[k]}$  for  $k^{\text{th}}$  degree, are also conducted.

**Training details:** For fair comparison all the aforementioned experiments have the same optimization-related hyper-parameters, e.g., the layer initialization. The training is run for 120 epochs with batch size 128 and the SGD optimizer is used. The initial learning rate is 0.1, while the learning rate is multiplied with a factor of 0.1 in epochs 40, 60, 80, 100. Classification accuracy is utilized as the evaluation metric.

### 4.1. Image classification with residual blocks

The standard benchmarks of CIFAR10 (Krizhevsky et al., 2014), CIFAR100 (Krizhevsky et al.) and ImageNet (Russakovsky et al., 2015) are utilized to evaluate our framework on image classification. To highlight the impact of the degree of the polynomial, we experiment with first (ResNet), second (SENet and  $\Pi$ -net<sup>3</sup>) as well as higher-degree polynomials. PDC relies on eq. 4; that is, we do not assume shared factor matrices across the different degree terms.

The first experiment is conducted on CIFAR100. The ResNet18 and the respective SENet are the baselines, while the  $\Pi$ -net-ResNet is the main comparison method. To exhibit the efficacy of PDC, we implement various versions: (a) PDC-channels is the variant that retains the same channels as the original ResNet18, (b) PDC-param has approximate the same parameters as the corresponding baselines, (c) PDC-comp has the least parameters that can achieve a performance similar to the ResNet18 (which is achieved by reducing the channels), (d) the PDC which is the variant that includes both reduced parameters and increased performance with respect to ResNet18, (e) the higher-degree variants of  $\text{PDC}^{[3]}$  and  $\text{PDC}^{[4]}$  that modify the PDC such

<sup>3</sup>The default  $\Pi$ -net block is designed as second-degree polynomial. Higher-degree blocks are denoted with the symbol  $.^{[k]}$ .

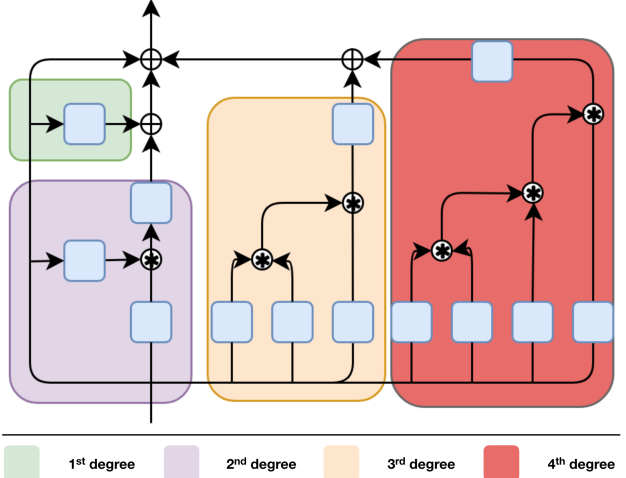


Figure 3. Illustration of the modular nature of the proposed polynomial expansion. Notice how we can trivially add new blocks in PDC to reach the pre-determined degree of the complete polynomial. The  $N^{\text{th}}$ -degree term includes  $N + 1$  new layers (i.e., blue boxes), which might make it impractical to expand over the fourth-degree. In practice, higher-degree polynomials make the model more expressive and hence allow for reduced number of channels.

that the degree of each respective block is three and four respectively (see Fig. 3).

The accuracy of each method is reported in Table 1. SENet improves upon the baseline of ResNet18, which verifies the benefit of second-degree correlations in the channels. This is further demonstrated with  $\Pi$ -net-ResNet that captures second-degree information on all dimensions and can achieve the same performance with reduced parameters. Our method can further reduce the parameters by 60% over ResNet18 and achieve the same accuracy. This can be attributed to the no-sharing scheme that enables more flexibility in the learned decompositions. The PDC-param further improves the accuracy by increasing the parameters, while the PDC-channels achieves the best accuracy by maintaining the same channels per residual block as ResNet18. The results exhibit that the expressive power of PDC can allow it to be used both for compression and for improving the performance by maintaining the same number of parameters.

The experiment is repeated with ResNet34 as the baseline. The accuracies in Table 2 demonstrate similar pattern, i.e., the parameters can be substantially reduced without sacrificing the accuracy.

A similar experiment is conducted on CIFAR10. The same networks as above are used as baselines, i.e., ResNet18 and SENet. The methods  $\Pi$ -net-ResNet and the PDC variants are also implemented as above. The results in Table 3 verify that both the  $\Pi$ -net-ResNet and PDC-comp can compress

Table 1. Image classification on CIFAR100 with variants of ResNet18. The second column reports the number of parameters (in millions), while the third column the accuracy (mean and standard deviation over 5 runs).

Model	# param ( $\times 10^6$ )	Accuracy
ResNet18	11.2	0.756
SENet	11.6	0.760
II-net-ResNet	6.1	0.760
PDC-comp	<b>4.3</b>	0.760
PDC-channels	19.2	<b>0.773</b>
PDC-param	11.4	0.770
PDC	8.0	0.765
PDC <sup>[3]</sup>	16.8	0.766
PDC <sup>[4]</sup>	28.0	0.771

Table 2. Image classification on CIFAR100 with variants of ResNet34.

Model	# param ( $\times 10^6$ )	Accuracy
ResNet34	21.3	0.769
II-net-ResNet	14.7	0.769
PDC-channels	36.3	<b>0.774</b>
PDC	<b>10.5</b>	0.770

substantially the number of parameters required while retaining the same accuracy. More importantly, our method achieves a parameter reduction of 28% over II-net-ResNet.

Table 3. Image classification on CIFAR10.

Model	# param ( $\times 10^6$ )	Accuracy
ResNet18	11.2	0.945
SENet	11.5	0.946
II-net-ResNet	6.0	0.945
PDC	8.0	<b>0.946</b>
PDC-comp	<b>4.3</b>	0.945
ResNet34	21.3	0.948
II-net-ResNet	13.0	<b>0.949</b>
PDC	<b>10.5</b>	0.948

The last experiment is conducted on ImageNet. We resize all the images to  $64 \times 64$  to accelerate the training time. We maintain the same hyper-parameters as above, e.g., learning rates and schedules; the only difference is the random cropping performed in the training images<sup>4</sup>. The results in Table 4 reflect the patterns that emerged above. The proposed PDC can reduce the number of parameters required while retaining the same accuracy. The variant of PDC that has similar number of parameters to the baseline ResNet18

<sup>4</sup>Focusing on various augmentation techniques proposed in ImageNet is not the focus of our method, so we use only core transformations during training. Additional details along with the accuracy curves are deferred to the supplementary.

can achieve an increase in the accuracy.

Table 4. Image classification on ImageNet with resolution  $64 \times 64$ .

Model	# param ( $\times 10^6$ )	Accuracy
ResNet18	11.7	0.601
SENet	12.0	0.606
PDC-comp	<b>7.9</b>	0.602
PDC	11.7	<b>62.7</b>

## 4.2. Image classification with non-local blocks

In this section, an experimental comparison and validation is conducted with non-local blocks. The benchmark of CIFAR100 is selected, while ResNet18 is referred as the baseline. The original non-local network (NL) and the disentangled non-local (DNL) are the main compared methods from the literature. As a reminder we perform two extensions in DNL: i) we add a first-degree term (PDC-NL<sup>[3]</sup>), ii) we add a fourth degree term (PDC-NL<sup>[4]</sup>).

Table 5 contains the accuracy of each method. Notice that DNL improves upon the baseline NL, while PDC-NL<sup>[3]</sup> improves upon both DNL and NL. Interestingly, the fourth-degree variant, i.e., PDC-NL<sup>[4]</sup> outperforms all the compared methods by a considerable margin without increasing the number of parameters significantly. The results verify our intuition that the different polynomial terms enable additional flexibility to the model.

Table 5. Classification on CIFAR100 with non-local blocks.

Model	# param ( $\times 10^6$ )	Accuracy
ResNet18	11.2	0.756
NL	11.57	0.769
DNL	11.57	0.771
PDC-NL <sup>[3]</sup>	11.87	0.773
PDC-NL <sup>[4]</sup>	12.00	<b>0.779</b>

## 4.3. Audio classification

Besides image classification, we conduct a series of experiments on audio classification to test the generalization of the polynomial expansion in different types of signals. The popular dataset of Speech Commands (Warden, 2018) is selected as our benchmark. The dataset consists of 60,000 audio files containing a single word each. The total number of words is 35, while there are at least 1,500 different files for each word. Every audio file is converted into a mel-spectrogram of resolution  $32 \times 32$ .

The accuracy for each model is reported in Table 6. All the compared methods have accuracy over 0.97, while the polynomial expansions of II-net-ResNet and PDC are able to reduce the number of parameters required to achieve the same accuracy, due to their expressiveness.

Table 6. Speech classification with ResNet18 variants.

Model	# param ( $\times 10^6$ )	Accuracy
ResNet18	11.2	0.977
SENet	11.5	0.977
II-net-ResNet	<b>6.0</b>	0.977
PDC	8.0	<b>0.978</b>

The high accuracy raises the question whether baselines with less parameters could achieve the same performance as the proposed PDC. To that end, ResNet7 and SENet7 are implemented. ResNet7 includes one residual block per group, while ResNet18 includes two residual blocks per group. We utilize the same amount of residual blocks, but use a second-degree expansion in each to implement PDC7. Table 7 reports the accuracy of each model, which is still over 0.97. However, PDC7 can achieve the same performance as the baseline under a reduced number of parameters.

Table 7. Speech classification with ResNet7 variants. Four residual blocks are used in ResNet7 instead of eight of ResNet18. Nevertheless, the respective PDC7 can reduce even further the parameters to achieve the same performance.

Model	# param ( $\times 10^6$ )	Accuracy
ResNet7	4.9	0.974
SENet7	5.1	0.974
PDC7	<b>3.9</b>	<b>0.975</b>

#### 4.4. Image classification with limited data

A number of experiments is performed by progressively reducing the number of training samples per class. The number of samples is reduced uniformly from the original 5,000 down to 50 per class, i.e., a  $100\times$  reduction, in CIFAR10. The architectures of Table 3 (similar to ResNet18) are used unchanged; only the number of training samples is progressively reduced. The resulting Fig. 4 visualizes the performance as we decrease the training samples. The accuracy of ResNet18 decreases fast for limited training samples. SENet deteriorates at a slower pace, steadily increasing the difference from ResNet18 (note that both share similar number of parameters). II-net-ResNet improves upon SENet and performs better even under limited data. However, the proposed PDC-comp outperforms all the compared methods for 50 training samples per class. The difference in the accuracy between PDC and II-net-ResNet increases as we reduce the number of training samples. Indicatively, with 50 samples per class, ResNet18 attains accuracy of 0.347, SENet scores 0.355, II-net-ResNet scores 0.397 and PDC-comp scores 0.426, which is a 22% increase over the ResNet18 baseline.

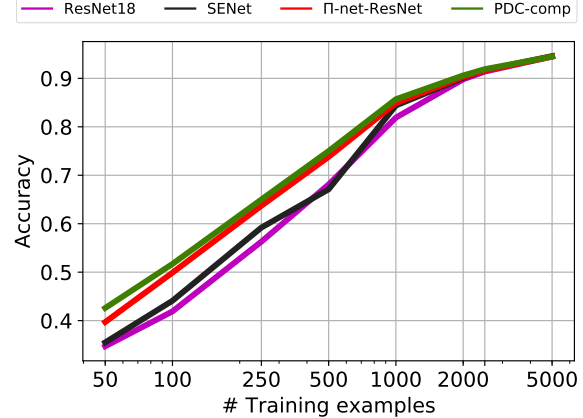


Figure 4. Image classification with limited data. The x-axis declares the number of training samples per class (log-axis). As the number of samples is reduced (i.e., moving from right to the left), the performance gap between II-net-ResNet and ResNet18 increases. Similarly, PDC-comp performs better than II-net-ResNet, especially in the limited data regimes on the left.

#### 4.5. Image classification on long-tailed distributions

The proposed models are scrutinized on long-tailed image recognition. We convert CIFAR10, which has 5,000 number of samples per class, to a long-tailed version, called CIFAR10-LT. The imbalance factor (IF) is defined as the ratio of the largest class to the smallest class. The imbalance factor varies from 10 – 200, following similar benchmarks tailored to long-tailed distributions (Cui et al., 2019). We note that the models are as defined above; the only change is the data distribution. The accuracy of each method is reported in Table 8. The results exhibit the benefits of the proposed models, which outperform the baselines.

Table 8. Accuracy on image classification on CIFAR10-LT. Each column corresponds to a different imbalance factor (IF).

Model \ IF	200	100	50	20	10
ResNet18	0.645	0.696	0.784	0.844	0.877
SENet	0.636	0.713	0.784	0.844	0.878
II-net-ResNet	0.653	0.718	0.783	0.845	0.879
PDC-comp	0.653	<b>0.727</b>	0.786	0.848	0.882
PDC-param	<b>0.665</b>	0.726	<b>0.792</b>	<b>0.851</b>	<b>0.886</b>

#### 5. Related work

Classification benchmarks (Russakovsky et al., 2015) have a profound impact in the progress observed in machine learning. Such benchmarks been a significant testbed for new architectures (Krizhevsky et al., 2012; He et al., 2016; Hu et al., 2018b) and for introducing novel tasks, such as adversarial perturbations (Szegedy et al., 2014). The

architectures originally designed for classification have been applied to diverse tasks, such as image generation (Brock et al., 2019; Zhang et al., 2019).

ResNet (He et al., 2016) has been among the most influential works of the last few years which can be attributed both in its simplicity and its stellar performance. ResNethas been studied in both its theoretical capacity (Hardt & Ma, 2017; Balduzzi et al., 2017; Shamir, 2018; Zaeemzadeh et al., 2018) and its empirical performance (Xie et al., 2017; Szegedy et al., 2017; Zagoruyko & Komodakis, 2016). A number of works focus on modifying the shortcut connection and the concatenation operation (Huang et al., 2017; Chen et al., 2017; Wang et al., 2018a).

The Squeeze-and-Excitation network(SENNet) (Hu et al., 2018b) has been extended by Roy et al. (2018) to capture second-degree correlations in both the spatial and the channel dimensions. (Hu et al., 2018a) extend SENNet by replacing the pooling operation with alternative operators that aggregate contextual information. Yang et al. (2020) inspired by the SENet propose a gated convolution module. Ruan et al. (2020) improve SENet by introducing long-range dependencies. SENet has also been used as a drop-in module to improve the performance of residual blocks (Gao et al., 2019).

Non-local neural networks have been used extensively for capturing long-range interactions in both image-related tasks (Li et al., 2020; Zhu et al., 2019; Huang et al., 2019) and video-related tasks (Chen et al., 2018; Girdhar et al., 2019). Non-local networks are also related with self-attention (Vaswani et al., 2017) that is widely used in both vision (Parmar et al., 2019) and natural language processing (Galassi et al., 2019; Ma et al., 2019). Cao et al. (2019) study when the long-range interactions emerge in non-local neural networks. They also frame a simplified non-local block, which in our terminology is a second-degree polynomial. Naturally, they observe that this resembles the SENet and merge their simplified non-local block and SENet block.

A promising line of research is that of polynomial activation functions. For instance, the element-wise quadratic activation function  $f^2$  applied to a linear operation  $C\hat{Z}$  is  $(C\hat{Z})^2$ . Both the theoretical (Kileel et al., 2019; Livni et al., 2014) and the empirical results (Ramachandran et al., 2017; Lokhande et al., 2020) support that polynomial activation functions can be beneficial. Our work is orthogonal to the polynomial activation functions, as they express a polynomial expansion of the representation, while we model a polynomial expansion of the input.

A well-established line of research is that of considering second or higher-order moments for various tasks. For instance, second-order statistics have been used for normalization methods (Huang et al., 2018), learning latent variable mod-

els (Anandkumar et al., 2014). However, our work focuses on classification methods that can be expresses as polynomials and not on the method of moments.

Tensors and tensor decompositions are related to our work (Sidiropoulos et al., 2017). Tensor decompositions such as the CP or the Tucker decompositions (Kolda & Bader, 2009) are frequently used for model compression in computer vision. Tensor decompositions have also been used for modeling the components of deep neural networks. Cohen & Shashua (2016) interpret a whole convolutional network as a tensor decomposition, while the recent Einconv (Hayashi et al., 2019) focus on a single convolutional layer and model them with tensor decompositions. In our work the focus is not in the tensor decomposition used, but on the polynomial expansion that provides insights on the correlations that are captured by each model.

A line of research that is related to ours is that of multiplicative data fusion (Jayakumar et al., 2020; Georgopoulos et al., 2020; Reed et al., 2014; Yu et al., 2017; Kim et al., 2018). Even though multiplicative interactions can be considered as second-degree polynomials, data fusion of the aforementioned works is not our focus.

## 6. Conclusion

In this work, we study popular classification networks under the unifying perspective of polynomials. Notably, the popular ResNet, SENet and non-local networks are expressed as first, second and third degree polynomials respectively. The common framework provides insights on the inductive biases of each model and enables natural extensions building upon their polynomial nature. We conduct an extensive evaluation on image and audio classification benchmarks. We show how intuitive extensions to existing networks, e.g., converting the third-degree non-local network into a fourth degree, can improve the performance. Such natural extensions can be used for designing new architectures based on the proposed taxonomy. Importantly, our experimental evaluation highlights the dual utility of the polynomial framework: the networks can be used either for model compression or increased model performance. We expect this to be a significant feature when designing architectures for edge devices. Our experimentation in the presence of limited data and long-tailed data distributions highlights the benefits of the proposed taxonomy and provides a link to real-world applications, where massive data annotation is challenging.

## References

Anandkumar, A., Ge, R., Hsu, D., Kakade, S. M., and Telgarsky, M. Tensor decompositions for learning latent variable models. *Journal of Machine Learning Research*,

15:2773–2832, 2014.

Balduzzi, D., Frean, M., Leary, L., Lewis, J., Ma, K. W.-D., and McWilliams, B. The shattered gradients problem: If resnets are the answer, then what is the question? In *International Conference on Machine Learning (ICML)*, pp. 342–350, 2017.

Brock, A., Donahue, J., and Simonyan, K. Large scale gan training for high fidelity natural image synthesis. In *International Conference on Learning Representations (ICLR)*, 2019.

Cao, Y., Xu, J., Lin, S., Wei, F., and Hu, H. Gcnet: Non-local networks meet squeeze-excitation networks and beyond. In *International Conference on Computer Vision Workshops (ICCV'W)*, pp. 0–0, 2019.

Chen, Y., Li, J., Xiao, H., Jin, X., Yan, S., and Feng, J. Dual path networks. In *Advances in neural information processing systems (NeurIPS)*, pp. 4467–4475, 2017.

Chen, Y., Kalantidis, Y., Li, J., Yan, S., and Feng, J.  $\hat{A^2}$ -nets: Double attention networks. In *Advances in neural information processing systems (NeurIPS)*, pp. 352–361, 2018.

Chrysos, G., Moschoglou, S., Bouritsas, G., Panagakis, Y., Deng, J., and Zafeiriou, S.  $\pi$ -nets: Deep polynomial neural networks. In *Conference on Computer Vision and Pattern Recognition (CVPR)*, 2020.

Cohen, N. and Shashua, A. Convolutional rectifier networks as generalized tensor decompositions. In *International Conference on Machine Learning (ICML)*, pp. 955–963. PMLR, 2016.

Cui, Y., Jia, M., Lin, T.-Y., Song, Y., and Belongie, S. Class-balanced loss based on effective number of samples. In *Conference on Computer Vision and Pattern Recognition (CVPR)*, pp. 9268–9277, 2019.

Galassi, A., Lippi, M., and Torroni, P. Attention, please! a critical review of neural attention models in natural language processing. *arXiv preprint arXiv:1902.02181*, 2019.

Gao, S., Cheng, M.-M., Zhao, K., Zhang, X.-Y., Yang, M.-H., and Torr, P. H. Res2net: A new multi-scale backbone architecture. *IEEE Transactions on Pattern Analysis and Machine Intelligence (T-PAMI)*, 2019.

Georgopoulos, M., Chrysos, G., Pantic, M., and Panagakis, Y. Multilinear latent conditioning for generating unseen attribute combinations. *International Conference on Machine Learning (ICML)*, 2020.

Girdhar, R., Carreira, J., Doersch, C., and Zisserman, A. Video action transformer network. In *Conference on Computer Vision and Pattern Recognition (CVPR)*, pp. 244–253, 2019.

Hanin, B. Universal function approximation by deep neural nets with bounded width and relu activations. *Mathematics*, 7(10):992, 2019.

Hardt, M. and Ma, T. Identity matters in deep learning. In *International Conference on Learning Representations (ICLR)*, 2017.

Hayashi, K., Yamaguchi, T., Sugawara, Y., and Maeda, S.-i. Einconv: Exploring unexplored tensor network decompositions for convolutional neural networks. In *Advances in neural information processing systems (NeurIPS)*, 2019.

He, K., Zhang, X., Ren, S., and Sun, J. Deep residual learning for image recognition. In *Conference on Computer Vision and Pattern Recognition (CVPR)*, 2016.

Hornik, K., Stinchcombe, M., White, H., et al. Multilayer feedforward networks are universal approximators. *Neural networks*, 2(5):359–366, 1989.

Hu, J., Shen, L., Albanie, S., Sun, G., and Vedaldi, A. Gather-excite: Exploiting feature context in convolutional neural networks. In *Advances in neural information processing systems (NeurIPS)*, pp. 9401–9411, 2018a.

Hu, J., Shen, L., and Sun, G. Squeeze-and-excitation networks. In *Conference on Computer Vision and Pattern Recognition (CVPR)*, pp. 7132–7141, 2018b.

Huang, G., Liu, Z., Van Der Maaten, L., and Weinberger, K. Q. Densely connected convolutional networks. In *Conference on Computer Vision and Pattern Recognition (CVPR)*, pp. 4700–4708, 2017.

Huang, L., Yang, D., Lang, B., and Deng, J. Decorrelated batch normalization. In *Conference on Computer Vision and Pattern Recognition (CVPR)*, pp. 791–800, 2018.

Huang, Z., Wang, X., Huang, L., Huang, C., Wei, Y., and Liu, W. Ccnet: Criss-cross attention for semantic segmentation. In *International Conference on Computer Vision (ICCV)*, pp. 603–612, 2019.

Jayakumar, S. M., Czarnecki, W. M., Menick, J., Schwarz, J., Rae, J., Osindero, S., Teh, Y. W., Harley, T., and Pascanu, R. Multiplicative interactions and where to find them. In *International Conference on Learning Representations (ICLR)*, 2020.

Kileel, J., Trager, M., and Bruna, J. On the expressive power of deep polynomial neural networks. In *Advances in neural information processing systems (NeurIPS)*, 2019.

Kim, J.-H., Jun, J., and Zhang, B.-T. Bilinear attention networks. In *Advances in neural information processing systems (NeurIPS)*, pp. 1564–1574, 2018.

Kolda, T. G. and Bader, B. W. Tensor decompositions and applications. *SIAM review*, 51(3):455–500, 2009.

Krizhevsky, A., Nair, V., and Hinton, G. Cifar-100 (canadian institute for advanced research). URL <http://www.cs.toronto.edu/~kriz/cifar.html>.

Krizhevsky, A., Sutskever, I., and Hinton, G. E. Imagenet classification with deep convolutional neural networks. In *Advances in neural information processing systems (NeurIPS)*, pp. 1097–1105, 2012.

Krizhevsky, A., Nair, V., and Hinton, G. The cifar-10 dataset. *online*: <http://www.cs.toronto.edu/~kriz/cifar.html>, 55, 2014.

Li, X., Wang, W., Hu, X., and Yang, J. Selective kernel networks. In *Conference on Computer Vision and Pattern Recognition (CVPR)*, pp. 510–519, 2019.

Li, Y., Jin, X., Mei, J., Lian, X., Yang, L., Xie, C., Yu, Q., Zhou, Y., Bai, S., and Yuille, A. L. Neural architecture search for lightweight non-local networks. In *Conference on Computer Vision and Pattern Recognition (CVPR)*, pp. 10297–10306, 2020.

Livni, R., Shalev-Shwartz, S., and Shamir, O. On the computational efficiency of training neural networks. In *Advances in neural information processing systems (NeurIPS)*, pp. 855–863, 2014.

Lokhande, V. S., Tasneeyapant, S., Venkatesh, A., Ravi, S. N., and Singh, V. Generating accurate pseudo-labels in semi-supervised learning and avoiding overconfident predictions via hermite polynomial activations. In *Conference on Computer Vision and Pattern Recognition (CVPR)*, pp. 11435–11443, 2020.

Ma, X., Zhang, P., Zhang, S., Duan, N., Hou, Y., Zhou, M., and Song, D. A tensorized transformer for language modeling. In *Advances in neural information processing systems (NeurIPS)*, pp. 2232–2242, 2019.

Nikol'skii, S. *Analysis III: Spaces of Differentiable Functions*. Encyclopaedia of Mathematical Sciences. Springer Berlin Heidelberg, 2013. ISBN 9783662099612.

Parmar, N., Ramachandran, P., Vaswani, A., Bello, I., Levskaya, A., and Shlens, J. Stand-alone self-attention in vision models. In *Advances in neural information processing systems (NeurIPS)*, pp. 68–80, 2019.

Ramachandran, P., Zoph, B., and Le, Q. V. Searching for activation functions. *arXiv preprint arXiv:1710.05941*, 2017.

Reed, S., Sohn, K., Zhang, Y., and Lee, H. Learning to disentangle factors of variation with manifold interaction. In *International Conference on Machine Learning (ICML)*, pp. 1431–1439, 2014.

Rolnick, D. and Tegmark, M. The power of deeper networks for expressing natural functions. In *International Conference on Learning Representations (ICLR)*, 2018.

Roy, A. G., Navab, N., and Wachinger, C. Concurrent spatial and channel ‘squeeze & excitation’ in fully convolutional networks. In *International conference on medical image computing and computer-assisted intervention*, pp. 421–429. Springer, 2018.

Ruan, D., Wen, J., Zheng, N., and Zheng, M. Linear context transform block. In *AAAI*, pp. 5553–5560, 2020.

Russakovsky, O., Deng, J., Su, H., Krause, J., Satheesh, S., Ma, S., Huang, Z., Karpathy, A., Khosla, A., Bernstein, M., et al. Imagenet large scale visual recognition challenge. *International Journal of Computer Vision (IJCV)*, 115(3):211–252, 2015.

Shamir, O. Are resnets provably better than linear predictors? In *Advances in neural information processing systems (NeurIPS)*, pp. 507–516, 2018.

Sidiropoulos, N. D., De Lathauwer, L., Fu, X., Huang, K., Papalexakis, E. E., and Faloutsos, C. Tensor decomposition for signal processing and machine learning. *IEEE Transactions on Signal Processing*, 65(13):3551–3582, 2017.

Simonyan, K. and Zisserman, A. Very deep convolutional networks for large-scale image recognition. In *International Conference on Learning Representations (ICLR)*, 2015.

Stone, M. H. The generalized weierstrass approximation theorem. *Mathematics Magazine*, 21(5):237–254, 1948.

Szegedy, C., Zaremba, W., Sutskever, I., Bruna, J., Erhan, D., Goodfellow, I., and Fergus, R. Intriguing properties of neural networks. In *International Conference on Learning Representations (ICLR)*, 2014.

Szegedy, C., Ioffe, S., Vanhoucke, V., and Alemi, A. A. Inception-v4, inception-resnet and the impact of residual connections on learning. In *AAAI Conference on Artificial Intelligence*, 2017.

Vaswani, A., Shazeer, N., Parmar, N., Uszkoreit, J., Jones, L., Gomez, A. N., Kaiser, Ł., and Polosukhin, I. Attention is all you need. In *Advances in neural information processing systems (NeurIPS)*, pp. 5998–6008, 2017.

Wang, W., Li, X., Yang, J., and Lu, T. Mixed link networks. In *International Joint Conferences on Artificial Intelligence (IJCAI)*, 2018a.

Wang, X., Girshick, R., Gupta, A., and He, K. Non-local neural networks. In *Conference on Computer Vision and Pattern Recognition (CVPR)*, pp. 7794–7803, 2018b.

Warden, P. Speech commands: A dataset for limited-vocabulary speech recognition. *arXiv preprint arXiv:1804.03209*, 2018.

Won, M., Chun, S., and Serra, X. Toward interpretable music tagging with self-attention. *arXiv preprint arXiv:1906.04972*, 2019.

Xie, S., Girshick, R., Dollár, P., Tu, Z., and He, K. Aggregated residual transformations for deep neural networks. In *Proceedings of the IEEE conference on computer vision and pattern recognition*, pp. 1492–1500, 2017.

Yang, Z., Zhu, L., Wu, Y., and Yang, Y. Gated channel transformation for visual recognition. In *Conference on Computer Vision and Pattern Recognition (CVPR)*, pp. 11794–11803, 2020.

Yin, M., Yao, Z., Cao, Y., Li, X., Zhang, Z., Lin, S., and Hu, H. Disentangled non-local neural networks. In *European Conference on Computer Vision (ECCV)*, 2020.

Yu, Z., Yu, J., Fan, J., and Tao, D. Multi-modal factorized bilinear pooling with co-attention learning for visual question answering. In *Proceedings of the IEEE international conference on computer vision*, pp. 1821–1830, 2017.

Zaeemzadeh, A., Rahnava, N., and Shah, M. Norm-preservation: Why residual networks can become extremely deep? *arXiv preprint arXiv:1805.07477*, 2018.

Zagoruyko, S. and Komodakis, N. Wide residual networks. *arXiv preprint arXiv:1605.07146*, 2016.

Zhang, H., Goodfellow, I., Metaxas, D., and Odena, A. Self-attention generative adversarial networks. In *International Conference on Machine Learning (ICML)*, 2019.

Zhu, Z., Xu, M., Bai, S., Huang, T., and Bai, X. Asymmetric non-local neural networks for semantic segmentation. In *International Conference on Computer Vision (ICCV)*, pp. 593–602, 2019.